Protein Structure

Deutsche Ausgabe: DOI: 10.1002/ange.201511609
Internationale Ausgabe: DOI: 10.1002/anie.201511609

Weak and Transient Protein Interactions Determined by Solid-State NMR

*Hugh R. W. Dannatt, Michele Felletti, Stefan Jehle, Yao Wang, Lyndon Emsley, Nicholas E. Dixon, Anne Lesage, and Guido Pintacuda**

Abstract: *Despite their roles in controlling many cellular processes, weak and transient interactions between large structured macromolecules and disordered protein segments cannot currently be characterized at atomic resolution by X-ray crystallography or solution NMR. Solid-state NMR does not suffer from the molecular size limitations affecting solution NMR, and it can be applied to molecules in different aggregation states, including non-crystalline precipitates and sediments. A solid-state NMR approach based on high magnetic fields, fast magic-angle sample spinning, and deuteration provides chemical-shift and relaxation mapping that enabled the characterization of the structure and dynamics of the transient association between two regions in an 80 kDa protein assembly. This led to direct verification of a mechanism of regulation of E. coli DNA metabolism.*

Transient and/or weak interactions involving protein segments that are intrinsically poorly structured are significant in the formation and stabilization of protein complexes.[1] Structural details of interactions of this type are difficult to elucidate. There is an inherent challenge in crystallizing such complexes,[2] and solution nuclear magnetic resonance (NMR) methods are restricted by molecular size, a particular problem for large multiprotein assemblies.[3]

High-resolution solid-state (ss) NMR under magic-angle spinning (MAS) is applicable to molecules that tumble slowly or are fully immobilized, and the spectral resolution is not affected by size.[4] Fast non-denaturing precipitation or sedimentation by centrifugation overcomes the need for protein crystals,[5] providing hydrated solids that retain the functional interactions from solution. ssNMR has a unique ability to complement the determination of protein structures with data on dynamics,[6] spanning wide timescales (10^{-11} to 10^{-3} s).

[*] Dr. H. R. W. Dannatt, M. Felletti, Dr. S. Jehle, Prof. L. Emsley, Dr. A. Lesage, Dr. G. Pintacuda
Centre de RMN à Très Hauts Champs—Université de Lyon
Institut de Sciences Analytiques (CNRS/ ENS-Lyon/ UCB Lyon 1)
69100 Villeurbanne (France)
E-mail: guido.pintacuda@ens-lyon.fr
Y. Wang, Prof. N. E. Dixon
Centre for Medical and Molecular Bioscience, School of Chemistry
University of Wollongong
Wollongong, New South Wales 2522 (Australia)
Prof. L. Emsley
Institut des Sciences et Ingénierie Chimiques, Ecole Polytechnique Fédérale de Lausanne, 1015 Lausanne (Switzerland)

Supporting information for this article can be found under: http://dx.doi.org/10.1002/anie.201511609.

A leap forward in ssNMR has been the advent of probes suitable for fast MAS (60 kHz and above).[7] Combined with perdeuteration and high magnetic fields, fast spinning allows the measurement of 2D ssNMR amide fingerprints of proteins with minimal signal overlap.[8] These developments speed up the backbone resonance assignment,[9] structure determination,[10] and dynamic description[10b,11] of microcrystalline proteins, and vastly increase the scope of ssNMR as a method for accessing more complex biological systems.[12] Herein, we show that these approaches provide a powerful platform to extend the techniques commonly used in solution NMR[2] to the study of weak and transient interactions in large, non-crystalline, or poorly soluble macromolecular complexes. In this study, we target the bacterial replisome, a widely studied dynamic multiprotein complex,[13] focusing on transient complexes involved in assembly at single-stranded DNA (ssDNA). These processes involve an intrinsically unstructured binding site in each subunit of the homotetrameric ssDNA-binding protein (SSB).[13c,14]

Bacterial SSBs bind to ssDNA in a sequence-independent manner,[15] protecting it from degradation or annealing to complementary sequences, whilst recruiting many other proteins to the ssDNA.[14] Each 177 amino acid subunit of the *E. coli* SSB (Figure S1) is comprised of a structured N-terminal ssDNA-binding (oligonucleotide binding, OB) domain (residues 1–115), followed by an unstructured[16] and generally poorly conserved C-domain. At the extreme C terminus (SSB-Ct, residues 170–177) is a highly conserved acidic motif (DFDDDIPF)[17] that is the site for the interaction of SSB with most of its partner proteins, including those in the replisome.[13c,14,17,18]

Crystal structures of the SSB OB domains have been determined with and without bound ssDNA, thereby allowing modeling of the complex in its two major DNA binding modes.[19] Information concerning the C-terminal domain, however, is at lower resolution, and no electron density has been reliably observed beyond residue Gly114.[16,20]

Nevertheless, the Ct motif and the OB domain interact in an autoinhibitory manner. The affinity of SSB for ssDNA is increased in an SSBΔCt mutant,[14,21] and binding of the Ct to accessory proteins is inhibited by the OB domain. An isolated Ct peptide has higher affinity for the PriA helicase and the χ subunit of DNA polymerase III than the complete SSB molecule, and high affinity is restored when SSB is bound to ssDNA.[14,20,22] Mass spectrometry studies have shown that the rate of subunit exchange in SSB is increased by removing the Ct, which is consistent with an interaction in trans between the Ct of one subunit and a region in a neighboring OB domain,[23] and solution NMR on monomeric SSB under low-

pH conditions identified intramolecular NOEs between Asp173 and Val29 and between Phe171 and Val58, thus providing structural evidence that the Ct binds back into the ssDNA-binding site.[16]

Together, these observations led to the hypothesis that the SSB-Ct motif binds the OB domain in the DNA binding groove, thereby competing with binding to ssDNA and reducing its ability to bind partner proteins in the absence of ssDNA. In this study, we used high magnetic field strengths, fast sample spinning, and proton-detected ssNMR experiments to characterize the structure and dynamics of the transient complex between the SSB-Ct and OB domains at physiological pH values on functional SSB tetramers.

We first observed by simple dialysis experiments in Tris-HCl buffers at various concentrations that *E. coli* SSB shows minimal solubility (ca. 0.2 mg mL^{-1}) in approximately 70 mM Tris, pH 8.0 in the absence of DNA; the protein precipitate can be recovered by centrifugation as a clear gel-like solid. These buffer conditions apparently favor interactions between ordered and disordered regions of neighboring tetramer units, thereby leading to multimerization of the tetramers to produce insoluble aggregates.

Figure 1 a,b shows 2D spectra of the SSB hydrogel, uniformly labeled with ^{2}H, ^{13}C, and ^{15}N, and reprotonated at all amide sites. The spectra correlate the chemical shifts of ^{1}H-^{15}N spin pairs in backbone amides and sidechains, in a manner similar to HSQC in solution NMR. Two types of correlations can be acquired on a solid sample, those using dipolar-coupling-based cross-polarization (CP) magnetization-transfer schemes ("CP-HSQC", Figure 2 a) and those using scalar-based magnetization-transfer steps (*J*-HSQC, Figure 2 b).

Assignment of the SSB signals can be readily transferred from those of protonated SSB[24] (Figure S2) with the help of a 3D experiment[8a] correlating the chemical shifts of ^{1}H, ^{15}N, and ^{13}CA nuclei ("CP-HNCA"). This yielded assignments of amide resonances of 63 residues in the OB domain (Table S1 in the Supporting Information), with none beyond Q110 being visible.[24] Three other regions were not detected, corresponding to loops with high *B*-factors in the X-ray structures (residues 22–27, 40–49, and 86–90).

CP-HSQC spectra show only peaks from rigid, ordered regions, since disorder leads either to inhomogeneous broadening of resonances or to motional averaging of dipolar couplings and reduced ^{1}H-^{15}N magnetization transfer in backbone amides. *J*-HSQC is complementary to CP-HSQC, since it detects correlations between spins with long coherence lifetimes, corresponding to rigid residues or to portions of the molecule undergoing fast isotropic motion.

Very few new resonances appeared in the *J*-HSQC spectrum (Figure 1 b), with most of those observed belonging to residues from the OB domain that are also visible in the CP-HSQC spectrum. The absence of most of the C-domain resonances, and notably all of those of the SSB Ct, from both of these spectra demonstrates that although the C-domain is indeed unstructured, it is not freely mobile in the SSB hydrogel. This supports the notion that interaction between the OB and C-domains gives rise to a disordered, "fuzzy" complex.[1]

Changes in the behavior of the C-domain in the complex with ssDNA were probed using SSB bound to Pf1 phage ssDNA; the large size of this complex allowed use of sedimentation to obtain a ssNMR sample.[25] Remarkably, the *J*-HSQC spectrum of the ssDNA complex (Figure 1 c) contains many of the expected signals that were missing from the spectra of SSB (Figure 1 b). These could be assigned on the basis of solution NMR assignments[16] and amongst them are resonances from residues in the Ct. By contrast, owing to SSB binding natural ssDNA with different DNA sequences bound to the OB domains, the CP-HSQC spectrum of the ssDNA complex is poorly resolved (Figure S3 in the Supporting Information). These spectra demonstrate that the C-domain is only freely flexible upon binding of ssDNA by the OB domain. Not all C-domain non-proline resonances are visible in the *J*-HSQC spectrum, which may indicate that some of the C-domain remains less mobile even in the presence of ssDNA.

To further probe the interaction between the C-terminal and OB domains, we used a mutant (SSBΔC8) that lacks the Ct, and observed changes in the OB-domain resonances compared to those of wild-type (wt) SSB. The CP-HSQC spectra of both samples contained similar, although not identical signals, thus confirming that the overall structure of the OB domain is not altered by C-terminal truncation (Figure 2 a). Since the chemical-shift differences

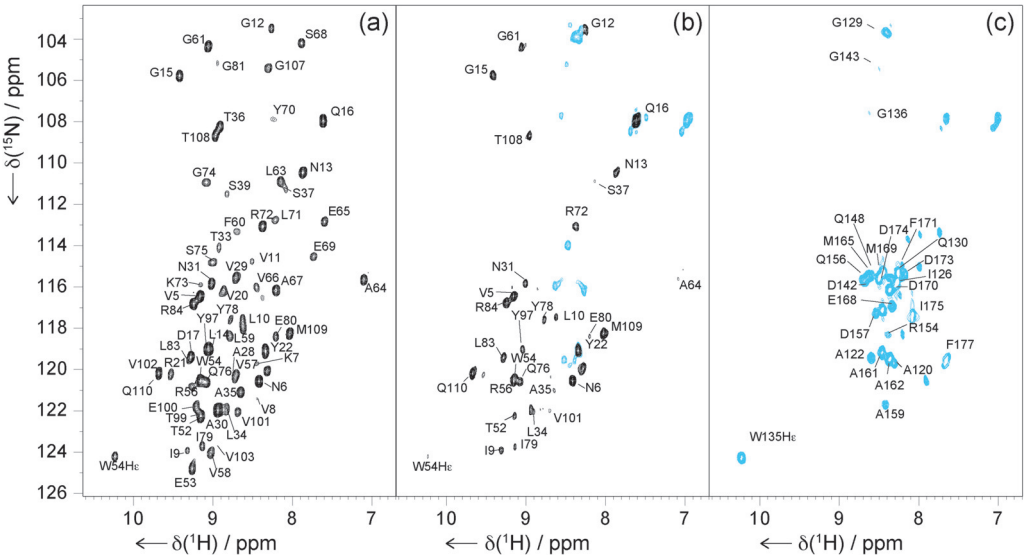

Figure 1. ^{1}H-^{15}N HSQC spectra of ^{1}H^{N},^{2}H,^{13}C,^{15}N-labeled wt *E. coli* SSB recorded at 1000 MHz with 60 kHz MAS. A CP-HSQC spectrum of the apoprotein (a), a *J*-HSQC spectrum of the apoprotein (b), and a J-HSQC spectrum of the SSB:ssDNA complex (c) are shown. In panel (b), the signals also present in the CP-HSQC spectrum (rigid regions) are shown in black, while new signals (mobile regions) are shown in blue.

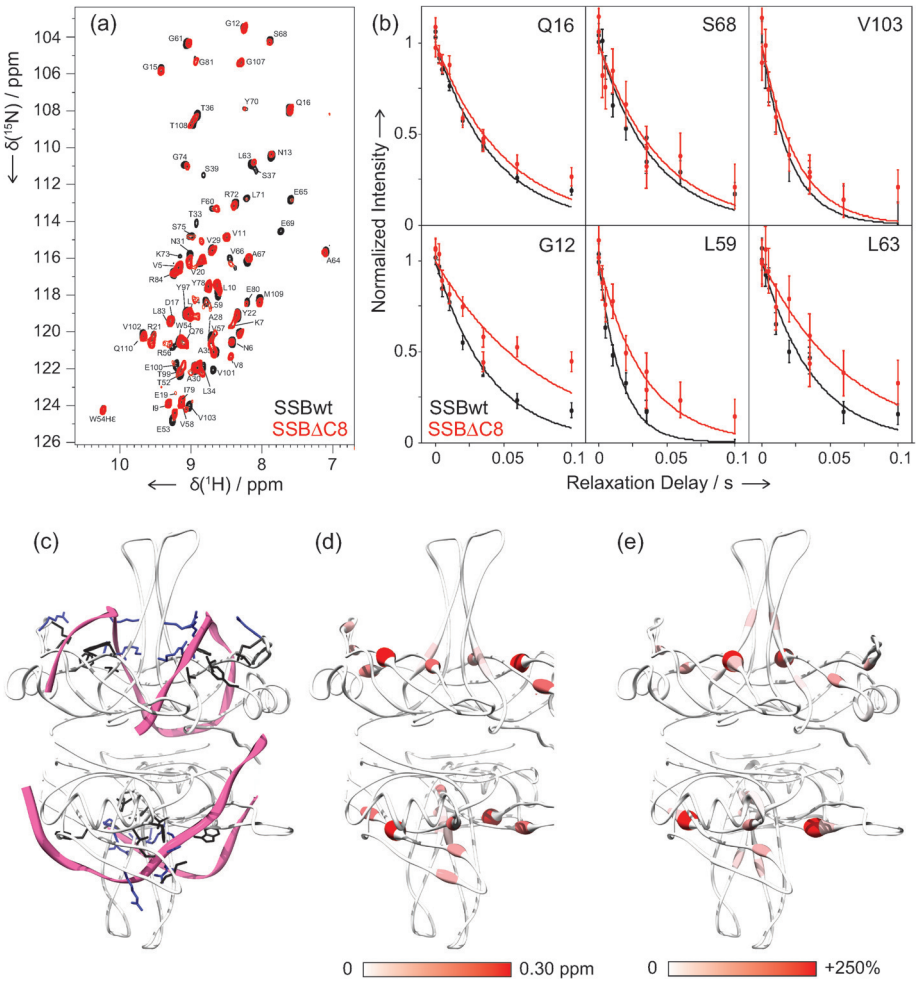

Figure 2. a) An overlay of the ^{1}H-^{15}N CP-HSQC spectra from the wild-type SSB (black) and SSBΔC8 (red) samples recorded at 1000 MHz with 60 kHz MAS. b) ^{15}N $R_{1\rho}$ relaxation-decay curves for wt SSB (black) and the SSBΔC8 mutant (red). The top row shows examples of three residues that gave ^{15}N $R_{1\rho}$ relaxation rates within error, whilst the bottom row gives examples of residues with significantly different rates between the samples. c) Crystal structure of the SSB tetramer (PDB ID: 1EYG[19b]), with the protein backbone shown as a white ribbon model and the ssDNA strands shown as pink ribbon models. Key residues involved in forming electrostatic (blue) and hydrophobic base-stacking (black) interactions are shown as stick models. d) An SSB backbone ribbon model colored to indicate the location and magnitude of chemical-shift perturbations between full-length SSB and SSBΔC8, with the largest differences shown in red. e) An SSB backbone ribbon model colored to show the relative increase in $R_{1\rho}$ values from ΔC8 to wt SSB.

were small, the CP-HNCA spectra of both samples allowed the assignment of backbone resonances from the wt sample to be transferred to the ΔC8 spectra (Table S2, Figure S4, S5). In addition, triple-resonance experiments allowed the chemical-shift perturbations (CSPs) resulting from deletion of the SSB Ct to be followed across C, H, and N backbone nuclei.[26] Although the CSP values (Table S3) are relatively small (< 0.31 ppm), residues with larger CSPs clustered in the DNA binding groove of the OB domain (Figure 2c–d). This directly indicates that there is an interaction between the conserved Ct motif and the OB domain, and that this interaction occurs directly at the DNA binding groove.

ssNMR also allows comment on the nature of the interaction between the SSB-Ct and the DNA binding groove. Since nuclear relaxation is strongly affected by molecular motion, site-specific ^{15}N relaxation rates complement the CSP measurements[12b,g] by identifying differences in dynamics between SSB and SSBΔC8, in particular when exploiting recently developed ^{1}H-detected ssNMR experiments at fast MAS.[10b,11a,c] Although the differences in chemical shifts between the samples caused different groups of signals to overlap between the two sets of spectra, we were able to extract ^{15}N $R_{1\rho}$ relaxation rates for 37 signals that were present in both the wt and ΔC8 spectra (Table S4). Although most residues gave rates that were identical within error (in the range of 10–20 s^{-1} at an applied RF field strength of 20 kHz), there were large differences for a subset of them (examples in Figure 2b). In each case, it was the wt sample that gave the higher ^{15}N $R_{1\rho}$ values, and mirroring the CSP measurements, these residues are associated with the DNA binding groove (Figure 2e). We did not see any significant deviation in rates between spin-lock frequencies of 2–20 kHz, or any difference in bulk ^{15}N R_1 relaxation rates between the samples. The $R_{1\rho}$ relaxation enhancement of the DNA binding groove residues in the presence of the Ct motif indicate chemical exchange in the μs–ms range as a result of weak (i.e., with intermolecular K_D in the μM range)[27] associations of the Ct motif with the DNA binding groove that are suppressed in SSBΔC8. These transient interactions explain the small CSPs between wt SSB and ΔC8 as a weighted average of the free and bound chemical shifts in the residues of the DNA binding groove, with the chemical shift of the free species making a significant contribution. In the case of the Ct, dynamic disorder and reversibility of transient association with the DNA binding groove cause an absence of visible signals. It remains possible that other parts of the Ct domain are statically disordered; many residues still give no observable signals even in the presence of DNA.

In summary, we have shown that contemporary solid-state NMR techniques allow the site-specific identification of transient interactions in a non-crystalline multimeric assembly that controls aspects of DNA metabolism in *E. coli*. Specifically, we have provided structural evidence at the atomic level for a model proposed to explain the auto-inhibition of SSB,[16,21,22,27] in which the presence of SSB-bound ssDNA in the cell is signaled to the binding partners of

SSB to enable their involvement in processes involved in DNA replication, recombination, and repair.[14] In contrast to previous studies,[16] this was accomplished by using functional tetramers at physiological pH values.

We highlight the utility of advanced methodological developments in ssNMR for addressing biological problems on samples for which other structural biology methods are not readily applicable. The combination of chemical-shift perturbation and site-specific relaxation measurements presented herein is likely to allow the characterization at atomic resolution of transient/disordered contacts of high biological significance throughout the interactome.

Acknowledgements

We are grateful to Gottfried Otting for his helpful comments. We acknowledge support from the Agence Nationale de la Recherche (ANR10-BLAN-713-01), the Joint Research Activity within Research Infrastructures in the 7th Framework program of the EC (BioNMR, contract n. 261863), the IR-RMN-THC FR3050 CNRS, and the Australian Research Council (DP0984797).

Keywords: DNA replication · magic angle spinning · solid-state NMR · protein structure · protein–protein interactions

How to cite: *Angew. Chem. Int. Ed.* **2016**, *55*, 6638–6641
Angew. Chem. **2016**, *128*, 6750–6753

[1] P. Tompa, M. Fuxreiter, *Trends Biochem. Sci.* **2008**, *33*, 2–8.
[2] P. E. Wright, H. J. Dyson, *Nat. Rev. Mol. Cell Biol.* **2015**, *16*, 18–29.
[3] a) A. N. Volkov, J. A. R. Worrall, E. Holtzmann, M. Ubbink, *Proc. Natl. Acad. Sci. USA* **2006**, *103*, 18945–18950; b) G. M. Clore, J. Iwahara, *Chem. Rev.* **2009**, *109*, 4108–4139.
[4] L. Emsley, I. Bertini, *Acc. Chem. Res.* **2012**, *46*, 1912–1913.
[5] a) I. Bertini, C. Luchinat, G. Parigi, E. Ravera, B. Reif, P. Turano, *Proc. Natl. Acad. Sci. USA* **2011**, *108*, 10396–10399; b) C. Gardiennet, A. K. Schuetz, A. Hunkeler, B. Kunert, L. Terradot, A. Boeckmann, B. H. Meier, *Angew. Chem. Int. Ed.* **2012**, *51*, 7855–7858; *Angew. Chem.* **2012**, *124*, 7977–7980.
[6] J. R. Lewandowski, M. E. Halse, M. Blackledge, L. Emsley, *Science* **2015**, *348*, 578–581.
[7] a) L. B. Andreas, T. Le Marchand, K. Jaudzems, G. Pintacuda, *J. Magn. Reson.* **2015**, *253*, 36–49; b) A. Boeckmann, M. Ernst, B. H. Meier, *J. Magn. Reson.* **2015**, *253*, 71–79.
[8] a) M. J. Knight, et al., *Angew. Chem. Int. Ed.* **2011**, *50*, 11697–11701; *Angew. Chem.* **2011**, *123*, 11901–11905; b) A. J. Nieuwkoop, W. T. Franks, K. Rehbein, A. Diehl, U. Akbey, F. Engelke, L. Emsley, G. Pintacuda, H. Oschkinat, *J. Biomol. NMR* **2015**, *61*, 161–171.
[9] a) E. Barbet-Massin, et al., *J. Am. Chem. Soc.* **2014**, *136*, 12489–12497; b) S. Q. Xiang, V. Chevelkov, S. Becker, A. Lange, *J. Biomol. NMR* **2014**, *60*, 85–90; c) L. B. Andreas, et al., *J. Biomol. NMR* **2015**, *62*, 253–261; d) S. Wang, et al., *Chem. Commun.* **2015**, *51*, 15055–15058.
[10] a) M. Huber, S. Hiller, P. Schanda, M. Ernst, A. Boeckmann, R. Verel, B. H. Meier, *ChemPhysChem* **2011**, *12*, 915–918; b) M. J. Knight, A. J. Pell, I. Bertini, I. C. Felli, L. Gonnelli, R. Pierattelli, T. Herrmann, L. Emsley, G. Pintacuda, *Proc. Natl. Acad. Sci. USA* **2012**, *109*, 11095–11100; c) R. Linser, B. Bardiaux, L. B. Andreas, S. G. Hyberts, V. K. Morris, G. Pintacuda, M. Sunde, A. H. Kwan, G. Wagner, *J. Am. Chem. Soc.* **2014**, *136*, 11002–11010; d) V. Agarwal, et al., *Angew. Chem. Int. Ed.* **2014**, *53*, 12253–12256; *Angew. Chem.* **2014**, *126*, 12450–12453.
[11] a) M. Tollinger, A. C. Sivertsen, B. H. Meier, M. Ernst, P. Schanda, *J. Am. Chem. Soc.* **2012**, *134*, 14800–14807; b) S. H. Park, C. Yang, S. J. Opella, L. J. Mueller, *J. Magn. Reson.* **2013**, *237*, 164–168; c) P. Ma, J. D. Haller, J. Zajakala, P. Macek, A. C. Sivertsen, D. Willbold, J. Boisbouvier, P. Schanda, *Angew. Chem. Int. Ed.* **2014**, *53*, 4312–4317; *Angew. Chem.* **2014**, *126*, 4400–4405; d) S. Asami, J. R. Porter, O. F. Lange, B. Reif, *J. Am. Chem. Soc.* **2015**, *137*, 1094–1100.
[12] a) T. Sinnige, M. Daniels, M. Baldus, M. Weingarth, *J. Am. Chem. Soc.* **2014**, *136*, 4452–4455; b) J. M. Lamley, et al., *J. Am. Chem. Soc.* **2014**, *136*, 16800–16806; c) P. Schanda, S. Triboulet, C. Laguri, C. M. Bougault, I. Ayala, M. Callon, M. Arthur, J.-P. Simorre, *J. Am. Chem. Soc.* **2014**, *136*, 17852–17860; d) M. T. Eddy, Y. Su, R. Silvers, L. Andreas, L. Clark, G. Wagner, G. Pintacuda, L. Emsley, R. G. Griffin, *J. Biomol. NMR* **2015**, *61*, 299–310; e) L. B. Andreas, M. Reese, M. T. Eddy, V. Gelev, Q. Z. Ni, E. A. Miller, L. Emsley, G. Pintacuda, J. J. Chou, R. G. Griffin, *J. Am. Chem. Soc.* **2015**, in press; f) E. Barbet-Massin, C.-T. Huang, V. Daebel, S.-T. D. Hsu, B. Reif, *Angew. Chem. Int. Ed.* **2015**, *54*, 4367–4369; *Angew. Chem.* **2015**, *127*, 4441–4444; g) J. M. Lamley, C. Öster, R. A. Stevens, J. R. Lewandowski, *Angew. Chem. Int. Ed.* **2015**, *54*, 15374–15378; *Angew. Chem.* **2015**, *127*, 15594—15598.
[13] a) P. M. Schaeffer, M. J. Headlam, N. E. Dixon, *IUBMB Life* **2005**, *57*, 5–12; b) C. S. McHenry, *Annu. Rev. Biochem.* **2011**, *80*, 403–436; c) A. Robinson, R. J. Causer, N. E. Dixon, *Curr. Drug Targets* **2012**, *13*, 352–372.
[14] R. D. Shereda, A. G. Kozlov, T. M. Lohman, M. M. Cox, J. L. Keck, *Crit. Rev. Biochem. Mol. Biol.* **2008**, *43*, 289–318.
[15] R. R. Meyer, P. S. Laine, *Microbiol. Rev.* **1990**, *54*, 342–380.
[16] D. Shishmarev, Y. Wang, C. E. Mason, X. C. Su, A. J. Oakley, B. Graham, T. Huber, N. E. Dixon, G. Otting, *Nucleic Acids Res.* **2014**, *42*, 2750–2757.
[17] Z. Kelman, A. Yuzhakov, J. Andjelkovic, M. O'Donnell, *EMBO J.* **1998**, *17*, 2436–2449.
[18] a) D. Lu, J. L. Keck, *Proc. Natl. Acad. Sci. USA* **2008**, *105*, 9169–9174; b) E. Antony, E. Weiland, Q. Yuan, C. M. Manhart, N. Binh, A. G. Kozlov, C. S. McHenry, T. M. Lohman, *J. Mol. Biol.* **2013**, *425*, 4802–4819.
[19] a) S. Raghunathan, C. S. Ricard, T. M. Lohman, G. Waksman, *Proc. Natl. Acad. Sci. USA* **1997**, *94*, 6652–6657; b) S. Raghunathan, A. G. Kozlov, T. M. Lohman, G. Waksman, *Nat. Struct. Biol.* **2000**, *7*, 648–652.
[20] S. N. Savvides, S. Raghunathan, K. Futterer, A. G. Kozlov, T. M. Lohman, G. Waksman, *Protein Sci.* **2004**, *13*, 1942–1947.
[21] A. G. Kozlov, M. M. Cox, T. M. Lohman, *J. Biol. Chem.* **2010**, *285*, 17246–17252.
[22] A. G. Kozlov, J. M. Eggington, M. M. Cox, T. M. Lohman, *Biochemistry* **2010**, *49*, 8266–8275.
[23] C. E. Mason, S. Jergic, A. T. Y. Lo, Y. Wang, N. E. Dixon, J. L. Beck, *J. Am. Soc. Mass Spectrom.* **2013**, *24*, 274–285.
[24] A. Marchetti, et al., *Angew. Chem. Int. Ed.* **2012**, *51*, 10756–10759; *Angew. Chem.* **2012**, *124*, 10914–10917.
[25] I. Bertini, C. Luchinat, G. Parigi, E. Ravera, *Acc. Chem. Res.* **2013**, *46*, 2059–2069.
[26] M. P. Williamson, *Prog. Nucl. Magn. Reson. Spectrosc.* **2013**, *73*, 1–16.
[27] X.-C. Su, Y. Wang, H. Yagi, D. Shishmarev, C. E. Mason, P. J. Smith, M. Vandevenne, N. E. Dixon, G. Otting, *Biochemistry* **2014**, *53*, 1925–1934.

Received: December 14, 2015
Published online: April 21, 2016

